Taxol-resistant breast cancer cell-derived exosome-delivered miR-187-5p regulates the growth of breast cancer cells via ABCD2 and Wnt/β-catenin signaling

TIELI WU[1], DANDAN ZHU[2], XINGYI WU[3], NINGNING ZHANG[4] and QINGYUAN ZHANG[1]

[1]Department of Medical Oncology, Harbin Medical University Cancer Hospital, Harbin, Heilongjiang 150000; [2]Department of Medical Oncology, Daqing Oilfield General Hospital, Daqing, Heilongjiang 163000; [3]Department of Internal Medicine, Qiqihar First Factory Hospital; [4]School of Basic Medicine, Qiqihar Medical University, Qiqihar, Heilongjiang 161000, P.R. China

Received August 29, 2022; Accepted January 24, 2023

DOI: 10.3892/ol.2023.13705

Abstract. Acquired resistance to Taxol (TAX) contributes to clinical treatment failure and significantly reduces the survival rate of patients. The present study aimed to explore the effects of exosomal microRNA (miR)-187-5p on TAX resistance in breast cancer cells and its underlying mechanisms. Exosomes were isolated from MCF-7 and TAX-resistant MCF-7/TAX cells, and the miR-187-5p and miR-106a-3p levels of the cells and exosomes were determined using reverse transcription-quantitative polymerase chain reaction (RT-qPCR). Next, MCF-7 cells were treated with TAX for 48 h and either treated with exosomes or transfected with miR-187-5p mimics. Cell viability, apoptosis, migration, invasion and colony formation were determined using Cell Counting Kit-8, flow cytometry, Transwell and colony formation assays, and the expression levels of associated genes and proteins were detected by RT-qPCR and western blotting, respectively. Finally, a dual-luciferase reporter gene assay was performed to confirm the target of miR-187-5p. The results showed that miR-187-5p expression levels increased significantly in TAX-resistant MCF-7 cells and exosomes compared with normal MCF-7 cells and exosomes ($P<0.05$). However, miR-106a-3p was not detected in the cells or exosomes. Therefore, miR-187-5p was selected for subsequent experiments. A series of cell assays showed that TAX inhibited the viability, migration, invasion and colony formation of MCF-7 cells and promoted their apoptosis; however, these changes were reversed by resistant cell exosomes and miR-187-5p mimics. Additionally, TAX significantly upregulated ABCD2 and downregulated β-catenin, c-Myc and cyclin D1, whereas resistant exosomes and miR-187-5p mimics reversed the TAX-induced changes in expression. Finally, *ABCD2* was confirmed to directly bind with miR-187-5p. It may be concluded that TAX-resistant cell-derived exosomes delivering miR-187-5p may affect the growth of TAX-induced breast cancer cells by targeting ABCD2 and c-Myc/Wnt/β-catenin signaling.

Correspondence to: Dr Qingyuan Zhang, Department of Medical Oncology, Harbin Medical University Cancer Hospital, 150 Haping Road, Nangang, Harbin, Heilongjiang 150000, P.R. China
E-mail: 0566@hrbmu.edu.cn

Key words: breast cancer, Taxol, miR-187-5p/ABCD2, drug resistance, Wnt/β-catenin

Introduction

Breast cancer is among the most common invasive malignancies threatening the health of women worldwide (1). Despite the various breast cancer treatment strategies that have been developed, breast cancer remains the second leading cause of cancer-associated deaths in women (2). The American Cancer Society estimates that ~281,550 women were diagnosed with breast cancer and ~43,600 women succumbed to breast cancer in 2021 (3). Currently, the primary treatment for breast cancer is surgery combined with radiotherapy or chemotherapy (1). Chemotherapy is administered for the management of breast cancer prior to and following surgery (4). Taxanes, including Taxol (TAX), are used clinically as chemotherapeutic agents for the treatment of early and advanced metastatic breast cancer (5,6). However, long-term chemotherapy can cause patients to develop resistance to chemotherapeutic drugs such as TAX, which greatly limits the efficacy of chemotherapy and may lead to systemic treatment failure (7,8). Therefore, elucidation of the mechanism of resistance to TAX chemotherapy is necessary to overcome these limitations and improve the survival rate of patients with breast cancer.

Exosomes are carriers of proteins, lipids and nucleic acids, including microRNAs (miRNAs), mRNAs and DNA, as well other active metabolites (9), and have been reported to play important roles in intercellular communication (10). Crow *et al* (11) demonstrated that exosomes from platinum-resistant A2780 epithelial ovarian cancer cells became resistant via the promotion of epithelial-mesenchymal transition (EMT), which implies the importance of exosomes in cancer drug resistance. miRNAs, a class of non-coding RNA with a length of ~22 nucleotides, participate in multiple

biological processes, such as cell proliferation, metastasis, invasion, apoptosis and aging, by regulating the expression of mRNAs (12,13). Studies have indicated that exosomal miRNAs are involved in tumorigenesis, metastasis, tumor response to treatment and the pathogenesis of tumor drug resistance (14,15). A study by Fu *et al* (16) demonstrated that multidrug resistant Bel/5-FU cells delivered miR-32-5p to sensitive Bel7402 cells via exosomes and activated the PI3K/Akt pathway, which further induced multidrug resistance via the regulation of angiogenesis and EMT. Another study showed that miR-221 enrichment was closely associated with sorafenib resistance, and hepatocellular carcinoma-associated exosomes containing miR-221 induced sensitive cells to become sorafenib resistant via the modulation of caspase-3 and suppression of apoptosis (17). Additionally, Uhr *et al* (18) suggested that hsa-miR-187-5p and hsa-miR-106a-3p may be indicators of drug resistance in breast cancer, and TAX sensitivity may be associated with hsa-miR-556-5p. However, the roles of exosomal miRNAs and their underlying mechanisms in the TAX resistance of breast cancer require elucidation.

Therefore, in the present study, exosomes were isolated from normal MCF-7 breast cancer cells and TAX-resistant MCF-7 breast cancer cells, and then the miR-187-5p and miR-106a-3p levels in the cells and exosomes were determined. As miR-187-5p was significantly enriched in TAX-resistant cells and TAX-resistant cell-derived exosomes, MCF-7 cells were treated with TAX for 48 h and the effects of exosomal miR-187-5p on TAX resistance in breast cancer cells and the associated underlying mechanisms were investigated. The aim of the present study is to lay a foundation for the discovery of novel therapeutic targets and pathways to confront acquired resistance to TAX in breast cancer chemotherapy.

Materials and methods

Cell culture. Breast cancer cells (MCF-7; drug sensitive, DS) and TAX-resistant breast cancer cells (MCF-7/TAX; drug resistant, DR) were purchased from The Cell Bank of Type Culture Collection of The Chinese Academy of Sciences and Procell Life Science & Technology Co., Ltd., respectively. The MCF-7 and MCF-7/TAX cells were cultured in Dulbecco's modified Eagle's medium (DMEM; Thermo Fisher Scientific, Inc.) containing 10% fetal bovine serum (FBS; Thermo Fisher Scientific, Inc.) and 100 U/ml penicillin/100 μg/ml streptomycin (Thermo Fisher Scientific, Inc.), and maintained in an incubator containing 5% CO_2 at 37˚C.

Isolation and identification of exosomes. The MCF-7 and MCF-7/TAX cell lines at 80-90% confluence were washed with PBS three times. Then, the medium was replaced with DMEM containing Systembio Exosome-Depleted FBS (cat. no. EXO-FBS-50A-1; SBI System Biosciences). After being cultured for 48 h, the cell supernatants of the MCF-7 and MCF-7/TAX cells were collected and used for exosome isolation. Exosome isolation from the cell supernatant was performed at 4˚C as previously described (19). Briefly, the cell supernatant was centrifuged at 500 x g for 5 min and then at 2,000 x g for 30 min at 4˚C. Subsequently, the supernatant was obtained and mixed with an equal volume of pre-cooled 16% polyethylene glycol. The mixture was incubated at 4˚C overnight and centrifuged at 10,000 x g for 60 min at 4˚C. After removing the supernatant, the sediments were resuspended in 1 ml PBS and centrifuged at 120,000 x g for 70 min at 4˚C. After removing the supernatant, the sediments were resuspended in 100 μl PBS to form an exosome suspension.

A BCA protein assay kit (Thermo Fisher Scientific, Inc.) was then used to determine the exosome concentration according to the manufacturer's instructions. Based on the methods of Lee *et al* (20), transmission electron microscopy (TEM; JEOL, Ltd.) was used to visualize the morphology of the isolated exosomes. Thereafter, the particle size and distribution of the exosomes were examined by nanoparticle tracking analysis (NTA) using a NanoSight NS300 particle size analyzer (Malvern Panalytical, Ltd.) as previously described (21). Additionally, the protein expression levels of heat shock protein 70 (HSP70), tumor susceptibility gene 101 (TSG101) and CD9, which are exosome-specific markers, were detected by western blotting using their corresponding antibodies: Anti-HSP70 antibody (catalogue number, 10995-1-AP; 1:1,000; ProteinTech Group, Inc.), anti-TSG101 antibody (catalogue number, 28283-1-AP; 1:1,000; ProteinTech Group, Inc.) and anti-CD9 antibody (catalogue number, 20597-1-AP; 1:1,000; Abcam). Anti-calnexin antibody (catalogue number, 10427-2-AP; 1:1,000; ProteinTech Group, Inc.) was used to detect calnexin as a cell marker and anti-GAPDH antibody (catalogue number, 10494-1-AP; 1:2,000; ProteinTech Group, Inc.) was used to detect GAPDH as a loading control (22).

Co-culture of MCF-7/TAX cell-derived exosomes and MCF-7 cells. To determine the uptake of MCF-7/TAX cell-derived exosomes by MCF-7 cells, a PKH67 staining kit (PKH67GL-1KT; Sigma-Aldrich; Merck KGaA) was used to label the exosomes with a green fluorescent dye, according to the manufacturer's instructions. Briefly, 700 μl MCF-7/TAX cell-derived exosomes was added to 1,300 μl Diluent C, and then 2 ml Diluent C with 16 μl PKH67 was added. After mixing, the mixture was incubated at room temperature for 5 min. Then, 4 ml 1% bovine serum albumin (BSA) was added to eliminate the excess dye. After being centrifuged at 120,000 x g for 90 min at 4˚C, the sediments were resuspended in 300 μl PBS, thereby forming a suspension of PKH67-labeled MCF-7/TAX cell-derived exosomes.

MCF-7 cells were seeded into a 24-well plate at a density of $3x10^4$ cells/well and cultured overnight. The next day, the medium was changed to serum-free medium and 10 μl PKH67-labeled MCF-7/TAX cell-derived exosomes were added to the cells. After co-culture for 48 h, the cells were washed with PBS and fixed with 4% paraformaldehyde at room temperature for 20 min. After washing with PBS, the cells were treated with 0.1% Triton X-100 for 20 min at room temperature. After thrice washing with PBS, 3% BSA blocking solution was added and the cells were incubated at room temperature for 1 h. After washing, the cytoskeleton was stained with red fluorescence by the addition of actin red (Nanjing KeyGen Biotech Co., Ltd.) and incubation at room temperature in the dark for 20 min. After washing, mounting medium with DAPI (Thermo Fisher Scientific, Inc.) was added to seal the slides, and images of the cells were captured under a laser confocal scanning microscope (TCS SP8; Leica Microsystems, Inc.).

Cell transfection. Cell transfection was carried out according to the method described by Liao *et al* (23). In brief, MCF-7 cells were seeded in a 24-well plate at a density of $5x10^4$ cells/well and cultured overnight. miR-187-5p mimics (sense: 5'-GGC TACAACACAGGACCCGGGC-3', and antisense: 5'-CCG GGUCCUGUGUUGUAGCCTT-3') and negative control (NC) mimics (sense: 5'-UUCUCCGAACGUGUCACGUTT-3', and antisense: 5'-ACGUGACACGUUCGGAGAATT-3') were designed and provided by Yanzai Biotechnology (Shanghai) Co., Ltd. After reaching 70% confluence, the cells were transfected with 50 nM miR-187-5p mimics or NC mimics using Lipofectamine® 2000 (Thermo Fisher Scientific, Inc.), following the manufacturer's protocol. After 6 h of transfection, the medium was replaced with a complete medium and the cells were cultured for another 48 h at room temperature. Total RNA was extracted from the cells after transfection, and the cell transfection efficiency was assessed by measuring the level of miR-187-5p using reverse transcription-quantitative polymerase chain reaction (RT-qPCR). The primers used for miR-187-5p are shown in Table I.

Detection of cell viability using a Cell Counting Kit-8 (CCK-8) assay in different treatment groups. MCF-7 cells were seeded into a 96-well plate at a density of $5x10^4$ cells/well, and different concentrations of TAX (0, 0.1, 0.2, 0.4, 0.8, 1.6, 3.2 and 6.4 μg/ml) were used to treat the cells for 48 h. The viability of the MCF-7 cells was then determined to screen for the optimum concentration of TAX using a CCK-8 assay (Beyotime Institute of Biotechnology). Thereafter, the MCF-7 cells were divided into six groups: Control, TAX, TAX + MCF-7/TAX cell-derived exosomes (TAX + DR-Exo), TAX + MCF-7 cell-derived exosomes (TAX + DS-Exo), TAX + NC mimics and TAX + miR-187-5p mimics. With the exception of those in the control group, the cells were all treated with TAX for 48 h, and then the cells in the TAX + DR-Exo, TAX + DS-Exo, TAX + NC mimics and TAX + miR-187-5p mimics groups were treated with MCF-7/TAX cell-derived exosomes (final concentration, 10 μg/ml) or MCF-7 cell-derived exosomes (final concentration, 10 μg/ml), or transfected with NC mimics or miR-185-5p mimics, respectively. After culture for 24, 48 and 72 h, 10 μl CCK-8 reagent was added to each well and the cells were incubated for 4 h. Finally, the absorbance at 450 nm was measured using a microplate reader.

Cell apoptosis determined by flow cytometry. The apoptosis of MCF-7 cells was examined using an Annexin V-FITC/PI apoptosis assay kit (Beyotime Institute of Biotechnology), according to the manufacturer's recommendations. In brief, the cells in the various treatment groups were harvested and resuspended in 1X binding buffer (100 μl). Next, 5 μl FITC-Annexin V and 5 μl PI (50 μl/ml) were added to the cells, which were then incubated in the dark for 15 min. Next, 400 μl 1X binding buffer was added and a FACSCalibur flow cytometer (Becton-Dickinson and Company) was used to analyze the cells. The total apoptotic rate (early and late apoptosis) was calculated using CellQuest software (version 4; Becton, Dickinson and Company).

Cell migration, invasion and colony formation assays. Transwell assays were performed to determine the migration and invasion of MCF-7 cells. Transwell chambers (pore size, 8 μm; Guangzhou Jet Bio-Filtration Co., Ltd.) were used to analyze cell migration, whereas Transwell chambers coated with Matrigel at 37˚C for 3 h were used for cell invasion. The upper chamber contained 200 μl cell suspension ($4x10^4$ cells in DMEM) and the lower chamber contained 500 μl DMEM containing 10% FBS and 100 U/ml penicillin/100 μg/ml streptomycin. After 48 h of incubation at 37˚C, the chambers were removed and washed twice with PBS. The cells were fixed with 4% paraformaldehyde at room temperature for 20 min. After washing, the cells were stained with crystal violet (Beyotime Institute of Biotechnology) at room temperature for 20 min. After washing away the excess dye and drying, the stained cells were observed and photographed under a light microscope.

For colony formation, the cells were seeded into a 6-well plate at a density of 200 cells/well, and the cells with different treatments were cultured in an incubator at 37˚C for 14 days. When cell colonies were visible, the supernatant was discarded and the cells were washed twice with PBS. Next, 4% paraformaldehyde was added to fix the cells for 10 min at room temperature. The excess paraformaldehyde was then removed and the cells were stained with crystal violet at room temperature for 10 min. After washing and drying, images were captured and cell colonies were counted using ImageJ

Table I. Primer sequences.

Primer	Sequence (5'-3')
hsa-miR-187-5p	RT: GTCGTATCCAGTGCAGGGTC CGAGGTATTCGCACTGGATACGA CGCCCGG F: GCGGCTACAACACAGGAC
hsa-miR-106a-3p	RT: GTCGTATCCAGTGCAGGGTC CGAGGTATTCGCACTGGATACGA CGTAAGA F: GCCTGCAATGTAAGCACT
Downstream universal primer	GTGCAGGGTCCGAGGT
U6	F: CTCGCTTCGGCAGCACA R: AACGCTTCACGAATTTGCGT
ABCD2	F: AATGGACCAGATCGAGTGCTG R: TGGGATAGAGGGTTTTCAGAGC
β-catenin	F: AAAGCGGCTGTTAGTCACTGG R: CGAGTCATTGCATACTGTCCAT
c-Myc	F: CCTGGTGCTCCATGAGGAGAC R: CAGACTCTGACCTTTTGCCAGG
Cyclin D1	F: GCTGCGAAGTGGAAACCATC R: CCTCCTTCTGCACACATTTGAA
GAPDH	F: TGACAACTTTGGTATCGTGGA AGG R: AGGCAGGGATGATGTTCTGGA GAG

miR, microRNA; ABCD2, ATP binding cassette subfamily D member 2; F, forward; R, reverse; RT, reverse transcription.

software (version 1.47; National Institutes of Health). A colony was defined as >50 cells. Triplicate wells were analysed for each treatment group.

RT-qPCR. Total RNA was extracted from differently treated cells using the RNAiso Plus kit (Takara Bio, Inc.) and twice the volume of isopropanol. The purity and concentration of the extracted total RNA were determined using a microplate reader. Subsequently, the total RNA was reverse transcribed into cDNA using a PrimeScript™ II 1st Strand cDNA Synthesis Kit (Takara Bio, Inc.) following the manufacturer's instructions. For the analysis of miRNA levels, the stem-loop method was used, as previously reported (24), and U6 served as a reference gene. GAPDH was used as the reference gene for mRNA expression. RT-qPCR was performed with Power SYBR Green PCR Master Mix (Thermo Fisher) and using the Applied Biosystems 7500 thermocycler (Applied Biosystems). qPCR was initiated at 50˚C for 2 min and proceeded with 40 cycles at 95˚C for 2 min, 95˚C for 15 sec and 60˚C for 60 sec. The sequences of all primers are listed in Table I, and the relative levels of miR-187-5p, miR-106a-3p, ATP binding cassette subfamily D member 2 (*ABCD2*), β-catenin, c-Myc and cyclin D1 were calculated using the $2^{-\Delta\Delta Cq}$ method (25).

Western blotting. Total protein was isolated from differently treated cells using RIPA lysis buffer (Beyotime Institute of Biotechnology), and the total protein concentration was measured using a BCA protein assay kit. Subsequently, the protein samples (20 μg/lane) were separated using 10% SDS-PAGE, transferred to PVDF membranes and blocked with 5% skimmed milk. After blocking at 37˚C for 1 h, the membranes were incubated with anti-β-catenin (catalogue number, 17565-1-AP; 1:1,000), anti-c-Myc (catalogue number, 10828-1-AP; 1:1,000), anti-cyclin D1 (catalogue number, 26939-1-AP; 1:1,000) and anti-GAPDH (catalogue number, 10494-1-AP; 1:2,000) antibodies, all from ProteinTech Group, Inc., or the aforementioned anti-HSP70, anti-TSG101, anti-CD9 and anti-calnexin antibodies at 4˚C overnight. After washing, the membranes were incubated with goat anti-rabbit/mouse IgG (H+L)-HRP secondary antibody (catalogue number, 111-035-003/115-035-003; 1:5,000; Jackson ImmunoResearch Laboratories, Inc.) at 37˚C for 2 h. After washing with PBST (1,000 ml 1X PBS + 1 ml Tween-20) five times, the protein bands were visualized using a Millipore ECL system (Tanon Science & Technology Co., Ltd.). The protein bands were analyzed using Image-Pro Plus software (version 6.0; Media Cybernetics Imaging Technologies Inc.).

Dual-luciferase reporter gene assay. The TargetScan online tool (https://www.targetscan.org/vert_71/) was used to predict the target of miR-187-5p, and a dual-luciferase reporter gene assay was used to analyze the interaction between miR-187-5p and *ABCD2*. The miR-187-5p mimic and *ABCD2* 3'-untranslated region (3'-UTR) were synthesized by and purchased from Yanzai Biotechnology (Shanghai) Co., Ltd. The pGL3-basic vector was provided by Yanzai Biotechnology (Shanghai) Co., Ltd. and was used to construct reporter plasmids containing the *ABCD2* 3'-UTR (pGL3-ABCD2-WT) and a mutated *ABCD2* 3'-UTR (pGL3-ABCD2-MUT). Afterwards, the pGL3-basic vector, pGL3-ABCD2-WT or pGL3-ABCD2-MUT (500 ng) were co-transfected into 293T cells (National Collection of Authenticated Cell Cultures) with miR-187-5p mimic (100 nM) or NC mimic (100 nM) using Lipofectamine 2000, according to the manufacturer's instructions. After culture for 48 h, a dual-luciferase reporter system (Promega Corporation) was used to measure the luminescent signal in relative light units. *Renilla* luciferase activity was normalized to firefly luciferase activity.

Statistical analysis. Results are reported as the mean ± standard deviation of at least three independent samples. GraphPad Prism 5 (GraphPad Software, Inc.) was used to perform the statistical analyses. Comparisons among three or more groups were performed using one-way analysis of variance followed by Tukey's post hoc test to analyze the pairwise differences. $P<0.05$ was considered to indicate a statistically significant difference.

Results

Characterization of MCF-7 and MCF-7/TAX cell-derived exosomes. Exosomes isolated from MCF-7 and MCF-7/TAX cells were characterized using TEM, NTA and western blotting. The TEM results revealed that the morphology of the exosomes isolated from both types of cells was cup-shaped and approximately round with a diameter of ~100 nm (Figs. 1A and S1). NTA showed that the major peaks of the substances from the MCF-7 and MCF-7/TAX cells occurred at sizes of ~134 and 138 nm, respectively (Fig. 1B), which was in accordance with the size distribution of exosomes reported previously (26). Additionally, western blotting revealed that HSP70, TSG101 and CD9, which are exosome-specific markers, were all expressed in the exosomes (Fig. 1C). However, calnexin, which is specific for cells, was only expressed in the cell lysate and not expressed in the exosomes (Fig. 1C). These results indicate that exosomes were successfully isolated from the MCF-7 and MCF-7/TAX cells.

To observe the uptake of the exosomes isolated from MCF/TAX cells in MCF-7 cells, PKH67 was used to stain the exosomes green (Fig. S2), actin red was used to stain the cytoskeleton red and the MCF-7 cell nuclei were stained blue using DAPI. Following co-culture for 48 h, green fluorescence was observed in the MCF-7 cells (Fig. 1D), indicating that PKH67-labeled MCF-7/TAX cell-derived exosomes were taken up by MCF-7 cells after the co-culture.

Selection of miRNAs and cell transfection efficiency. With the aim of selecting miRNAs for subsequent study, a literature search was conducted, which indicated that miR-187-5p and miR-106a-3p are closely associated with TAX resistance (18). Therefore, miR-187-5p and miR-106a-3p were chosen for further validation. The relative level of miR-187-5p was significantly higher in MCF-7/TAX (DR) cells compared with MCF-7 (DS_ cells ($P<0.05$), and its level was also significantly higher in MCF-7/TAX cell-derived exosomes compared with MCF-7 cell-derived exosomes ($P<0.05$; Fig. 2A). However, miR-106a-3p was not detected in cells or exosomes (data not shown), which may be due to low abundance in this cell line. Therefore, miR-187-5p was selected for evaluation in subsequent experiments.

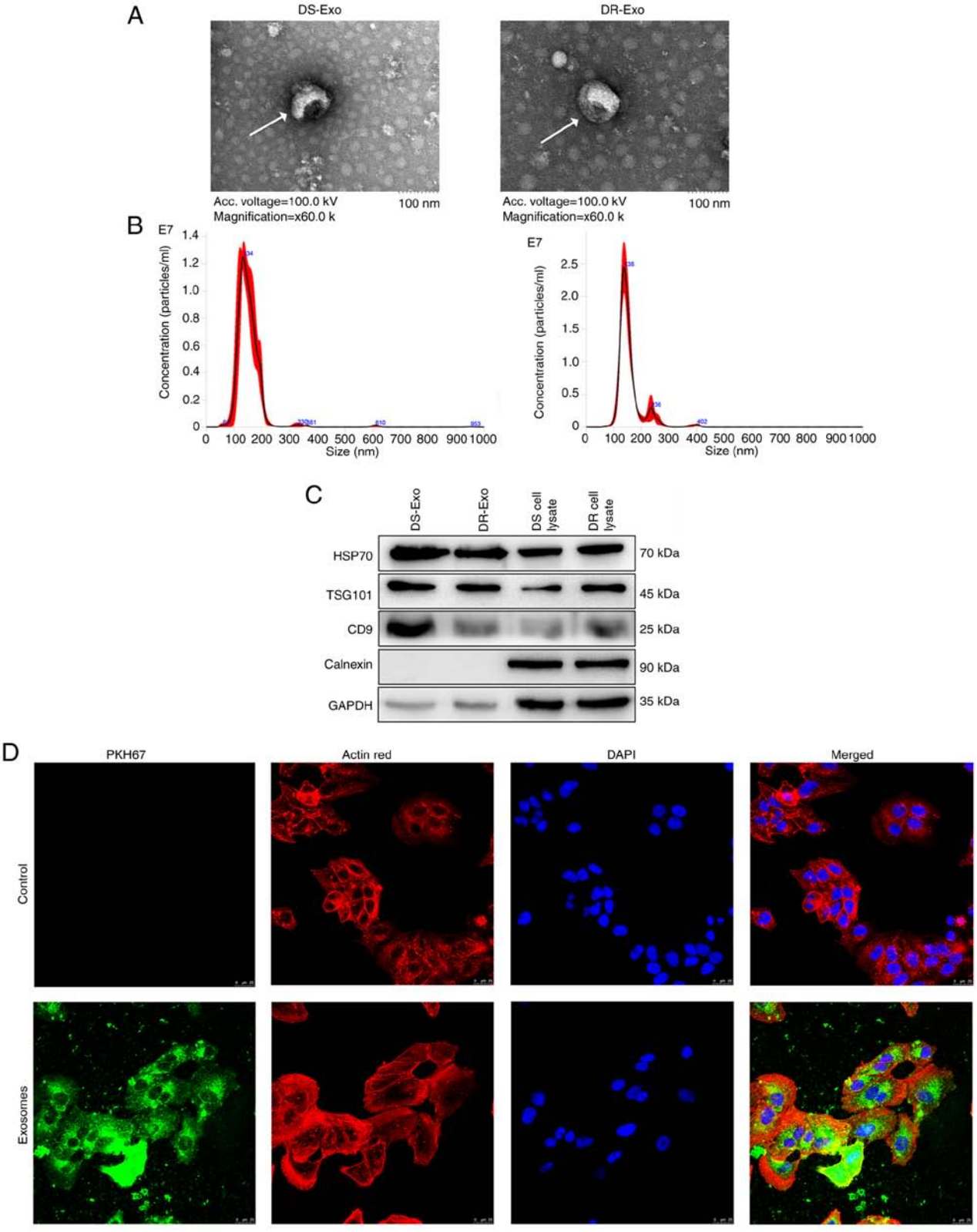

Figure 1. Characterization of exosomes isolated from MCF-7 cells and MCF-7/TAX cells. (A) Exosome morphology visualized by transmission electron microscopy. White arrows indicate exosomes. (B) Particle size distribution of the exosomes determined using a NanoSight NS300 particle size analyzer. (C) Expression levels of HSP70, TSG101, CD9 and calnexin in the exosomes and cell lysates detected by western blotting. (D) MCF-7/TAX cell-derived exosomes were labeled green with PKH67, actin red was used to stain the MCF-7 cytoskeleton and DAPI was used for nuclear staining. PKH67-labeled exosomes were taken up by MCF-7 cells after co-culture for 48 h at a magnification of x400. TAX, Taxol; DS, drug sensitive MCF-7; DR-Exo, drug resistant MCF/TAX; Exo, exosomes; HSP70, heat shock protein 70; TSG101, tumor susceptibility gene 101.

MCF-7 cells with miR-187-5p enrichment were constructed by transfection with miR-187-5p mimics, and the level of miR-187-5p was determined by RT-qPCR to evaluate the transfection efficiency. No significant difference in miR-187-5p

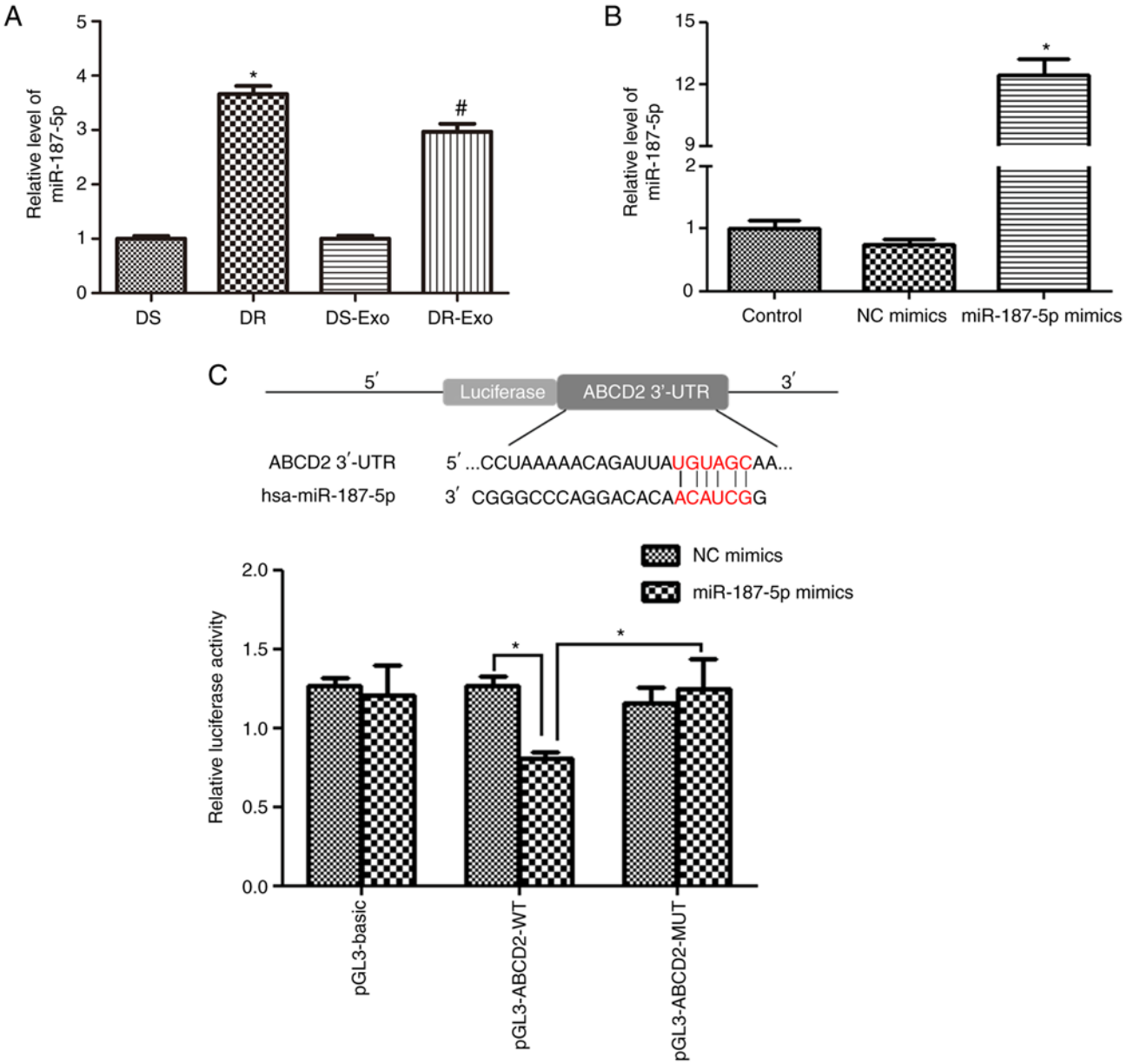

Figure 2. Cell transfection efficiency and the association between miR-187-5p and *ABCD2*. (A) Relative levels of miR-187-5p in cells and exosomes. *P<0.05 vs. the DS group; #P<0.05 vs. the DS-Exo group. (B) Cell transfection efficiency of MCF-7 cells evaluated by measuring the relative level of miR-187-5p. *P<0.05 vs. the control group. (C) *ABCD2* was confirmed to directly bind with miR-187-5p by a dual-luciferase reporter gene assay. *P<0.05 as indicated. DS, drug sensitive MCF-7 cells; DR, drug resistant MCF/TAX cells; Exo, exosomes; control, untransfected MCF-7 cells; NC, negative control; miR, microRNA; pGL3-basic, empty vector; pGL3-ABCD2-WT, wild-type 3'-UTR *ABCD2* reporter plasmid; pGL3-ABCD2-MUT, mutated 3'-UTR *ABCD2* reporter plasmid; UTR, untranslated region; ABCD2, ATP binding cassette subfamily D member 2.

levels was detected between the control and NC mimics groups (P>0.05; Fig. 2B). Compared with the control group, the relative level of miR-187-5p in the miR-187-5p mimics group was increased to 12.46±0.78, which was significantly elevated compared with that in the control and NC mimics groups (P<0.05; Fig. 2B). These results indicate that MCF-7 cells with miR-187-5p enrichment were successfully established and were suitable for further experiments.

ABCD2 directly binds with miR-187-5p. To explore the downstream regulatory mechanism of miR-187-5p, the online tool TargetScan was used to predict the target gene of miR-187-5p. *ABCD2* was identified as a potential target of miR-187-5p owing to the 3'-UTR of ABCD2 including a binding site for miR-187-5p (Fig. 2C). A dual-luciferase reporter gene assay was then performed to confirm the relationship between *ABCD2* and miR-187-5p. In the cells transfected with pGL3-basic vector, no significant difference was found in the relative luciferase activity between the NC mimics and miR-187-5p mimics (P>0.05; Fig. 2C). However, in the cells transfected with pGL3-ABCD2-WT, the relative luciferase activity was significantly reduced after co-transfection with miR-187-5p mimics compared with co-transfection with NC mimics (P<0.05). When *ABCD2* was mutated (pGL3-ABCD2-MUT plasmid), the relative luciferase activity after co-transfection with miR-187-5p mimics increased significantly compared with that observed for pGL3-ABCD2-WT and miR-187-5p mimics co-transfection (P<0.05), and was restored to a level similar to

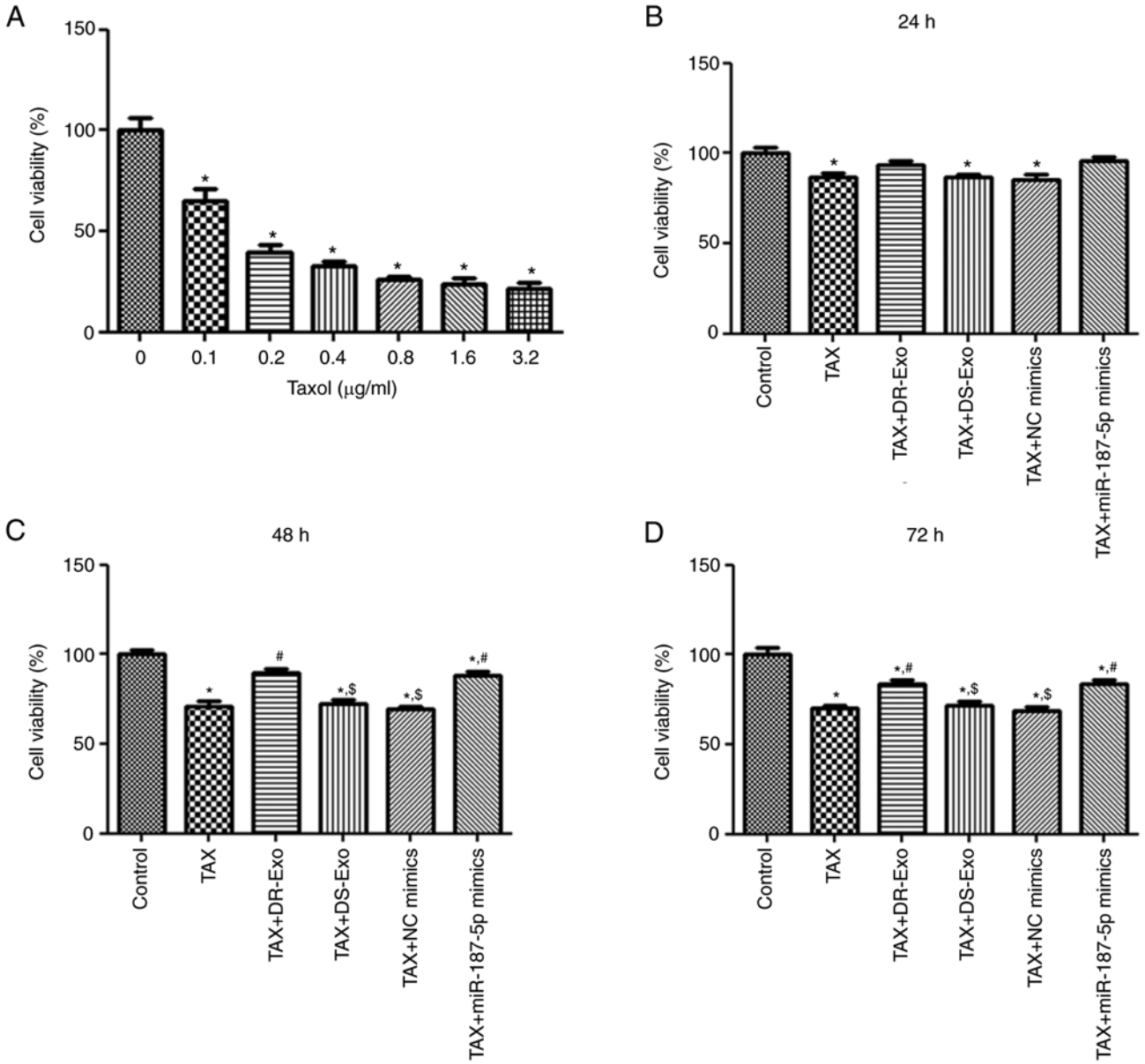

Figure 3. Screening for the optimal concentration of TAX, and the effects of exosomal miR-187-5p on the TAX-induced reduction of MCF-7 cell viability. (A) Viability of MCF-7 cells treated with different concentrations of TAX evaluated using a CCK-8 assay. *P<0.05 vs. the untreated control. Viability of MCF-7 cells with different treatments determined by CCK-8 after culture for (B) 24 h, (C) 48 h and (D) 72 h. The MCF-7 cells were treated with TAX for 48 h and various treatments or transfections were applied. *P<0.05 vs. the control group; #P<0.05 vs. the TAX group. $P<0.05 vs. the TAX + DR-Exo group. TAX, Taxol; miR, microRNA; CCK-8, Cell Counting Kit-8; control, untreated MCF-7 cells; DS-Exo, drug sensitive MCF-7 cell-derived exosomes; DR-Exo, drug resistant MCF/TAX cell-derived exosomes; NC, negative control.

that achieved with NC mimics (P>0.05; Fig. 2C). These results suggest that *ABCD2* directly binds to miR-187-5p.

Screening for the optimal TAX concentration and cell viability analysis. To determine the optimal TAX concentration, different concentrations of TAX were used to treat MCF-7 cells and the viability of the cells was measured using a CCK-8 assay. The viability of cells treated with TAX concentrations of 0.1, 0.2, 0.4, 0.8, 1.6 and 3.2 μg/ml was significantly lower than that of cells that did not receive TAX treatment (P<0.05; Fig. 3A). On the premise that MCF-7 cells treated with 0.1 μg/ml TAX had the highest viability among all the treatment groups, this concentration was selected for administration to the MCF-7 cells in subsequent experiments.

To understand the role of MCF-7/TAX cell-derived exosomal miR-187-5p in the viability of TAX-induced MCF-7 cells, the viability of TAX-induced MCF-7 cells that were treated with MCF-7/TAX cell-derived (DR) exosomes or transfected with miR-187-5p mimics was determined. After culture for 24 h, the viability of MCF-7 cells in the TAX, TAX + DS-Exo and TAX + NC mimics groups was significantly lower than that in the control group (P<0.05), while there was no significant difference in cell viability among the TAX, TAX + DR-Exo, TAX + DS-Exo and TAX + miR-187-5p mimics groups (P>0.05; Fig. 3B). After culture for 48 and 72 h, the cell viability of the TAX + DR-Exo and TAX + miR-187-5p mimics groups was significantly higher compared with that of the TAX group (P<0.05), and no significant differences were

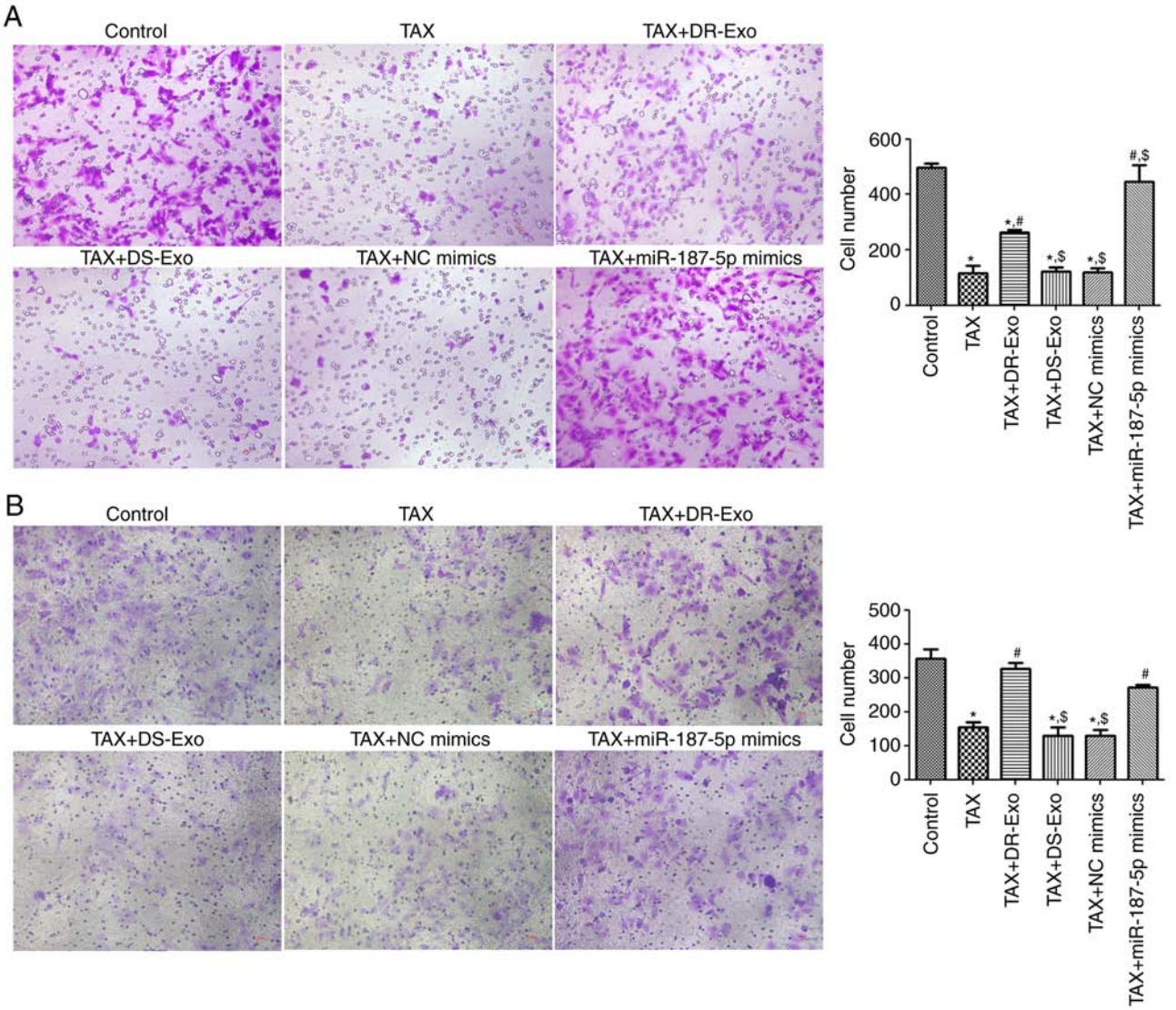

Figure 4. Effects of exosomal miR-187-5p on the TAX-induced migration and invasion of MCF-7 cells. The MCF-7 cells were treated with TAX for 48 h and various treatments or transfections were applied. (A) Migration of MCF-7 cells with different treatments evaluated using Transwell assays. The left panel shows representative images of crystal violet-stained migrated cells at a magnification of x200. The right panel shows the migrated cell number in the different groups. (B) Invasion of MCF-7 cells with different treatments examined using Transwell assays. The left panel shows representative images of crystal violet-stained invaded cells at a magnification of x200. The right panel shows the invaded cell number in the different groups. *P<0.05 vs. the control group; #P<0.05 vs. the TAX group; $P<0.05 vs. the TAX + DR-Exo group. miR, microRNA; TAX, Taxol; control, untreated MCF-7 cells; DS-Exo, drug sensitive MCF-7 cell-derived exosomes; DR-Exo, drug resistant MCF/TAX cell-derived exosomes; NC, negative control.

observed between the TAX + DR-Exo and TAX + miR-187-5p mimics, as well as among the TAX, TAX + DS-Exo and TAX + NC mimics groups (P>0.05; Fig. 3C and D). These results indicate that TAX inhibited the viability of MCF-7 cells, and that MCF-7/TAX cell-derived exosomes and miR-187-5p enrichment reversed the TAX-induced loss in viability of the MCF-7 cells.

Cell migration and invasion analyses. To investigate further the effects of MCF-7/TAX cell-derived exosomal miR-187-5p on the migration and invasion of TAX-induced MCF-7 cells, Transwell assays were performed to test the migration and invasion of MCF-7 cells induced by TAX. The numbers of migrated and invaded cells in the TAX group were significantly lower compared with those in the control group (P<0.05; Fig. 4). Compared with cells treated only with TAX, the numbers of migrated and invaded cells treated with MCF-7/TAX cell-derived exosomes or transfected with miR-187-5p mimics were significantly higher after TAX treatment (P<0.05), whereas the numbers of migrated and invaded cells did not change significantly following treatment with MCF-7 cell-derived exosomes or transfection with NC mimics (P>0.05; Fig. 4). In terms of migrated cells, the cell number in the TAX + miR-187-5p mimics group was significantly higher than that in the TAX + DR-Exo group (P<0.05; Fig. 4A). In terms of invaded cells, no significant difference in the cell number was detected between these two groups (P>0.05; Fig. 4B). These results imply that TAX suppressed the migration and invasion of MCF-7 cells, while MCF-7/TAX cell-derived exosomes and miR-187-5p enrichment attenuated the effects of TAX. In addition, the effects of miRNA-187-5p and DR-Exo of

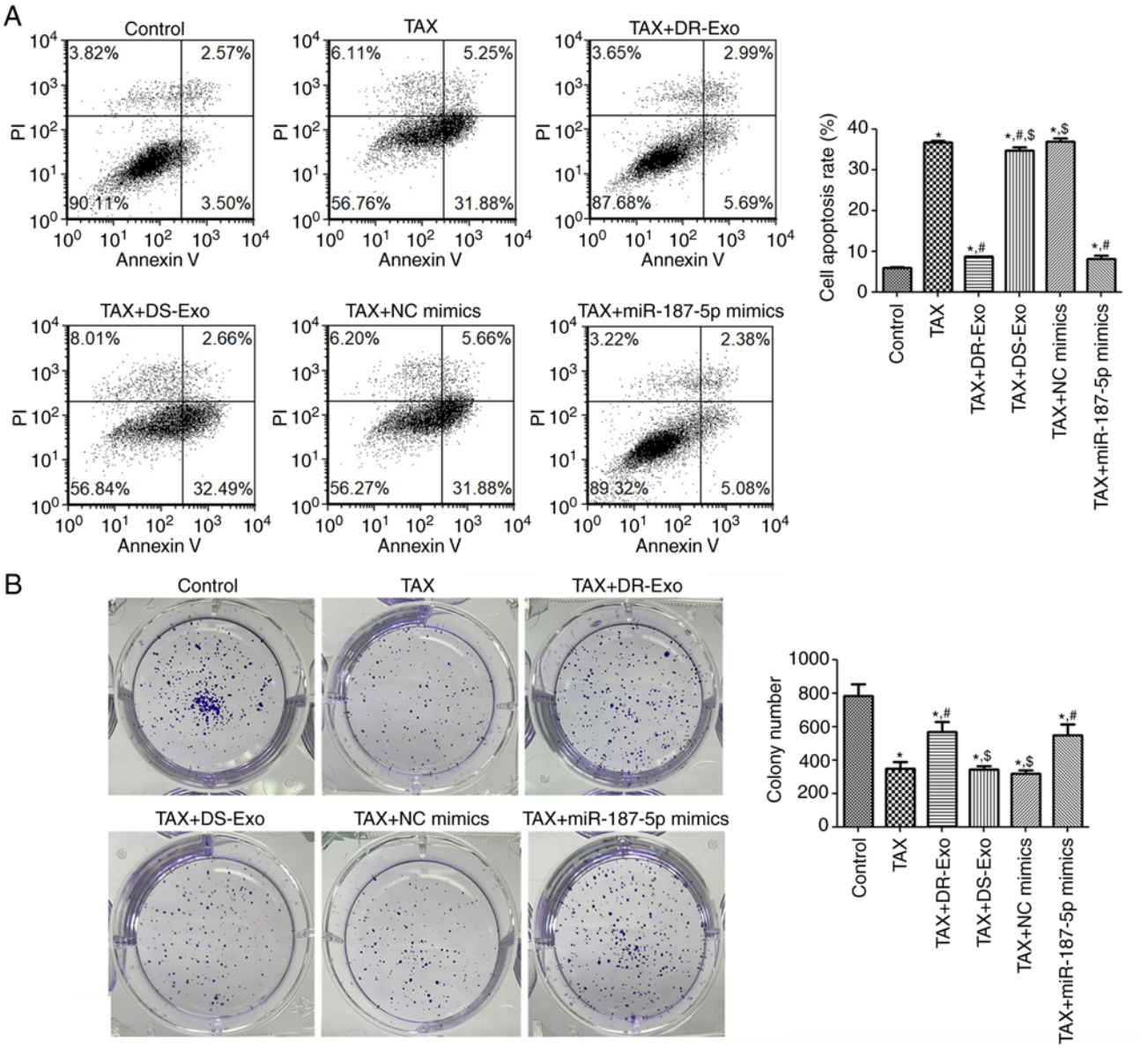

Figure 5. Effects of exosomal miR-187-5p on TAX-induced changes in the apoptosis and colony formation of MCF-7 cells. The MCF-7 cells were treated with TAX for 48 h and various treatments or transfections were applied. (A) Apoptosis of the MCF-7 cells with different treatments determined by flow cytometry. The left panel shows representative images acquired by flow cytometry. The right panel shows the cell apoptosis rate in the different groups. (B) Colony formation of MCF-7 cells following different treatments. The left panel shows representative images of colony formation. The right panel shows the number of colonies in each group. *P<0.05 vs. the control group; #P<0.05 vs. the TAX group; $P<0.05 vs. the TAX + DR-Exo group. miR, microRNA; TAX, Taxol; control untreated MCF-7 cells; DS-Exo, drug sensitive MCF-7 cell-derived exosomes; DR-Exo, drug resistant MCF/TAX cell-derived exosomes; NC, negative control.

MCF-7 cell growth may contribute to the difference in migration and invasion.

Cell apoptosis and colony formation analyses. The apoptosis of MCF-7 cells with different treatments was determined using flow cytometry to investigate the actions of MCF-7/TAX cell-derived exosomal miR-187-5p on the apoptosis of TAX-induced MCF-7 cells. The cell apoptosis rate was significantly enhanced after TAX treatment compared with that in the control group (P<0.05), and no significant difference was found in the cell apoptosis rate between the TAX and TAX + NC mimics groups (P>0.05; Fig. 5A). The MCF-7/TAX cell-derived exosomes, MCF-7 cell-derived exosomes and miR-187-5p mimics significantly reduced the TAX-induced cell apoptosis rate compared with that in the TAX group (P<0.05), with the reduction induced by the MCF-7/TAX cell-derived exosomes and miR-187-5p mimics being particularly evident (P<0.05; Fig. 5A). These results indicate that TAX induced the apoptosis of MCF-7 cells, whereas MCF-7/TAX cell-derived exosomes and miR-187-5p enrichment attenuated the apoptosis caused by TAX.

Thereafter, the colony formation of MCF-7 cells subjected to different treatments was examined. The number of MCF-7 cell colonies formed after treatment with TAX decreased significantly compared with that in the control group, (P<0.05; Fig. 5B). No significant differences in colony numbers were detected among the TAX, TAX + DS-Exo and TAX + NC mimics groups (P>0.05; Fig. 5B). In addition, the colony numbers in the TAX + DR-Exo and TAX + miR-187-5p mimics groups were significantly higher than those in the

TAX group (P<0.05), and significantly lower than those in the control group (P<0.05; Fig. 5B). These results show that TAX inhibited the colony formation of MCF-7 cells, whereas MCF-7/TAX cell-derived exosomal miR-187-5p promoted TAX-induced MCF-7 colony formation.

Effects of exosomal miR-187-5p on the expression of ABCD2, β-catenin, c-Myc and cyclin D1. To investigate the molecular mechanisms of exosomal miR-187-5p involvement in the TAX-induced effects on MCF-7 cells, the expression levels of ABCD2, β-catenin, c-Myc and cyclin D1 were determined using RT-qPCR and western blotting. RT-qPCR showed that TAX significantly upregulated *ABCD2* mRNA expression compared with that in the control group (P<0.05), and MCF-7 cell-derived exosomes and NC mimics did not significantly alter the increase in *ABCD2* mRNA expression caused by TAX (P>0.05; Fig. 6A). However, the *ABCD2* mRNA expression following TAX treatment was significantly downregulated by MCF-7/TAX cell-derived exosomes and miR-187-5p mimics compared with TAX alone (P<0.05), and was reduced to a level similar to that of the control group (P>0.05; Fig. 6A). The trend in β-catenin mRNA expression in the different groups was opposite to that of *ABCD2* mRNA expression (Fig. 6B). The mRNA expression of c-Myc was significantly downregulated after TAX treatment compared with that in the control group (P<0.05) and did not significantly change after treatment with MCF-7 cell-derived exosomes or NC mimics transfection compared with that in the TAX group (P>0.05; Fig. 6C). However, the mRNA expression of c-Myc was significantly upregulated by MCF-7/TAX cell-derived exosomes and miR-187-5p mimics compared with that in the TAX group (P<0.05), and the action of miR-187-5p mimics was significantly greater compared with that of the TAX + DR-Exo group (P<0.05; Fig. 6C). Cyclin D1 mRNA expression was significantly downregulated in the cells treated with TAX compared with that in the control group (P<0.05) and was also significantly downregulated in the TAX-induced cells treated with MCF-7 cell-derived exosomes and NC mimics (P<0.05); no significant differences were detected among the TAX, TAX + DS-Exo and TAX + NC mimics groups (P>0.05; Fig. 6D). However, when the TAX-induced cells were treated with MCF-7/TAX cell-derived exosomes or transfected with miR-187-5p mimics, cyclin D1 mRNA expression was significantly upregulated compared with that in cells only treated with TAX (P<0.05; Fig. 6D). Additionally, the protein levels of β-catenin, c-Myc and cyclin D1 were detected using western blotting, and representative protein bands are shown in Fig. 6E. The quantitative analysis showed that the trends in β-catenin, c-Myc and cyclin D1 protein expression in the different groups detected by western blotting were similar to those of β-catenin, c-Myc and cyclin D1 mRNA expression measured by RT-qPCR (Fig. 6F-H).

Discussion

Breast cancer is the most frequently occurring cancer in women and the second most common cancer worldwide (27). TAX is a first-line chemotherapeutic agent for the treatment of patients with breast cancer (28). However, long-term TAX chemotherapy causes patients with breast cancer to acquire TAX resistance (29), which contributes to clinical treatment failure and markedly reduces the survival rate. Exosomes, particularly tumor-derived exosomes, have been reported to deliver miRNAs that can confer drug resistance to target cells and play essential roles in the drug resistance of tumors (11,30). Therefore, in the present study, exosomes were extracted from MCF-7 and MCF-7/TAX cells so that their effects could be investigated. Western blotting showed that exosome-specific markers HSP70, TSG101 and CD9 were all expressed in the exosomes and cell lysate, which indicated that a large number of exosomes were present. The difference in the expression levels of CD9 observed between the exosomes and cell lysate may be due to the source of cells, and the presence of TAX. Based on the presence of these markers combined with the results of NTA and TEM, it can be inferred that exosomes were successfully isolated from MCF-7 and MCF-7/TAX cells. After that, the levels of miR-187-5p and miR-106a-3p were measured in the exosomes and cells. The results revealed that miR-187-5p was significantly enriched in MCF-7/TAX cells and MCF-7/TAX cell-derived exosomes, which indicated that the resistance MCF-7 cells to TAX was closely associated with miR-187-5p enrichment.

There is evidence that the exosome-mediated transfer of miRNAs alters the drug resistance of cancer cells, and is a potential biomarker for the progression and treatment of cancer (30). A study by Santos *et al* (31) showed that resistant cell-derived exosomes were enriched in miR-155, which inhibited the migration ability of breast cancer cells and promoted chemoresistance in sensitive cells by exosomal transfer. Another study indicated that tumor-associated macrophage-derived exosomes transmitted miR-21 to gastric cancer cells, which increased the cell viability and colony formation of the cancer cells and restrained their apoptosis, thus endowing them with cisplatin resistance (32). To explore the roles of MCF-7/TAX cell-derived exosomes in the delivery of miR-187-5p during the treatment of MCF-7 cells with TAX, MCF-7 cells were treated with TAX and then either treated with MCF-7/TAX cell-derived exosomes or transfected with miR-187-5p mimics. Treatment with TAX significantly inhibited the viability, migration, invasion and colony formation of MCF-7 cells and promoted their apoptosis. However, MCF-7/TAX cell-derived exosomes and miR-187-5p mimics reversed the TAX-induced changes in cell viability, apoptosis, migration, invasion and colony formation. Furthermore, the growth-inducing effects of miRNA-187-5p and MCF-7/TAX cells-derived exosomes on MCF-7 cells may increase their migration and invasion. TAX has been shown to be effective against various cancers via the repression of cancer cell viability and induction of apoptosis (33,34). Additionally, a study reported that miR-187-5p is an oncogene that increased the risk of recurrence in bladder cancer, while its overexpression promoted the proliferation and mobility of bladder cancer cells and repressed their apoptosis (35), implying that miR-187-5p may play an important role in the development of cancers. Based on the results of the present study, it may be speculated that TAX-resistant MCF-7 cell-derived exosomes regulate the growth of TAX-induced MCF-7 cells via the delivery of miR-187-5p, thus affecting the drug resistance of breast cancer cells.

A study by Hu *et al* (36) showed that exosomes secreted by colorectal cancer cells activated the Wnt/β-catenin signaling

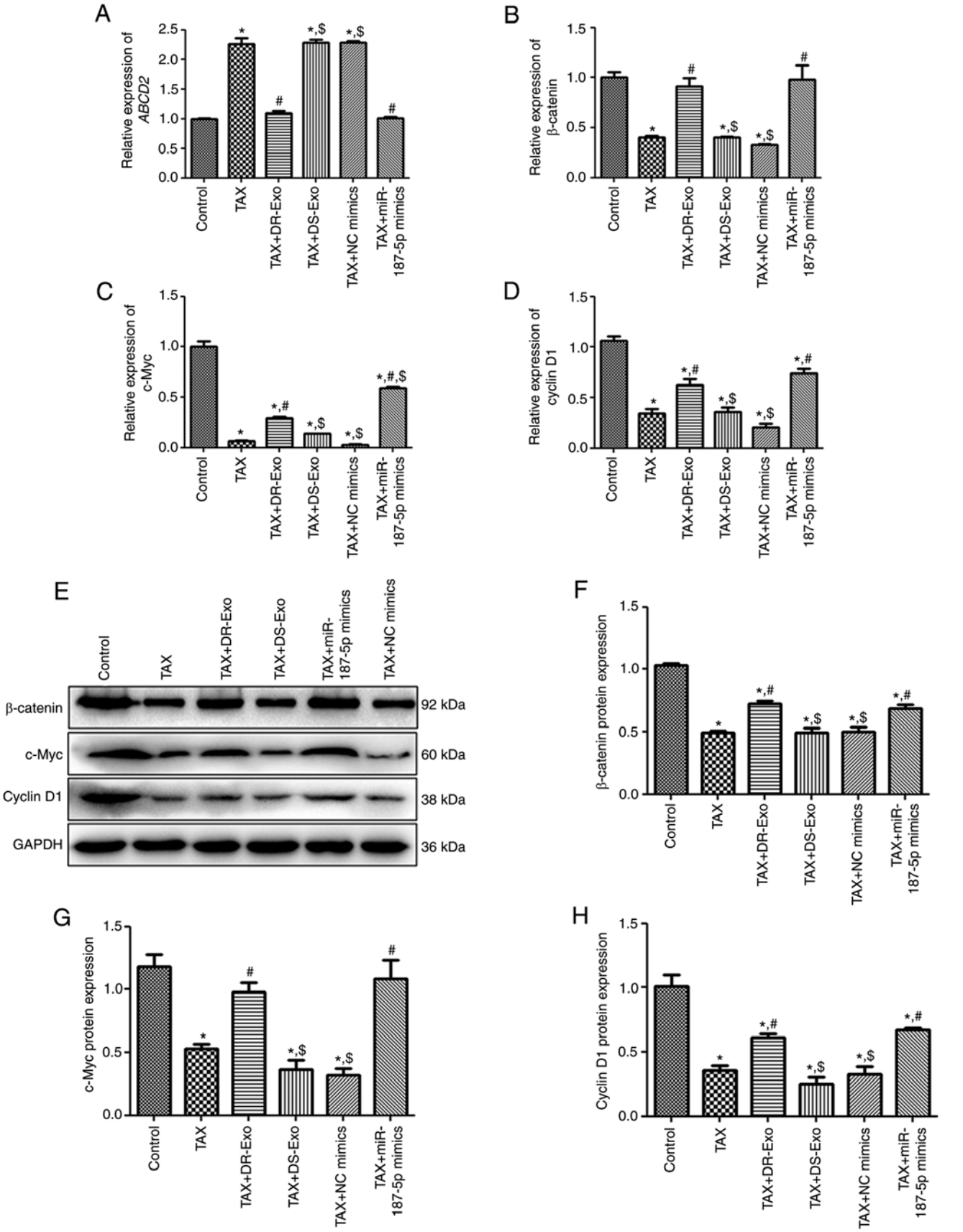

Figure 6. Effects of exosomal miR-187-5p on the expression of ABCD2, β-catenin, c-Myc and cyclin D1 in MCF-7 cells. MCF-7 cells were treated with TAX for 48 h and various treatments or transfections were applied. Relative mRNA expression of (A) *ABCD2*, (B) β-catenin, (C) c-Myc and (D) cyclin D1 in MCF-7 cells with different treatments determined by reverse-transcription-quantitative PCR. (E) Representative images of β-catenin, c-Myc and cyclin D1 western blots. Quantified protein levels of (F) β-catenin, (G) c-Myc and (H) cyclin D1 in MCF-7 cells with different treatments. *P<0.05 vs. the control group; #P<0.05 vs. the TAX group; $P<0.05 vs. the TAX + DR-Exo group. miR, microRNA; ABCD2, ATP binding cassette subfamily D member 2; TAX, Taxol; control, untreated MCF-7 cells; DS-Exo, drug sensitive MCF-7 cell-derived exosomes; DR-Exo, drug resistant MCF/TAX cell-derived exosomes; NC, negative control.

pathway by promoting the stabilization and nuclear translocation of β-catenin, resulting in resistance to 5-fluorouracil and oxaliplatin. Another study demonstrated that exosomes released from cisplatin-resistant A549 human lung cancer cells induced therapeutic resistance by upregulating mTOR expression (37). These reports suggest that exosomes affect various signal transduction pathways and thereby regulate drug resistance (30). Moreover, the Wnt/β-catenin signaling pathway, which induces EMT, invasion and metastasis, has been reported to serve an important role in the development and progression of breast cancer (38). Therefore, in the present study, the effects of the Wnt/β-catenin signaling pathway on TAX resistance in breast cancer were investigated. The results showed that TAX significantly upregulated ABCD2 and downregulated β-catenin, c-Myc and cyclin D1 expression compared with that in untreated MCF-7 cells, whereas the MCF-7/TAX cell-derived exosomes and miR-187-5p mimics significantly attenuated the effects of TAX. A dual-luciferase reporter gene assay confirmed that miR-187-5p directly bound to the *ABCD2* UTR. ATP-binding box (ABC) transporters promote the development of anticancer drug resistance via ATP-dependent drug efflux. ABCD2 is a type of ABC transporter protein that is overexpressed in patients with breast cancer receiving neoadjuvant chemotherapy (39) and is associated with the progression and prognosis of breast cancer (40). Overall, it can be inferred that TAX-resistant MCF-7 cell-derived exosomal miR-187-5p mediates TAX resistance in breast cancer cells via the direct targeting of ABCD2.

Park *et al* (41) reported that ABCD2 is a direct target of β-catenin, indicating that ABCD2 may be involved in the Wnt/β-catenin signaling pathway. β-catenin is the core transcription factor of the Wnt/β-catenin signaling pathway; it is a key factor in the transmission of signals to the nucleus and the initiation of Wnt-specific gene transcription, which may contribute to the specificity of various cells and tissues (42). Cyclin D1 is a target gene of the Wnt/β-catenin signaling pathway that drives cancer cell proliferation, and its activation is closely associated with poor clinical prognosis in breast cancer (43). Cyclin D1 is necessary for the proliferation of tamoxifen-resistant breast cancer cells, and its overexpression is associated with poor outcomes in patients with breast cancer treated with tamoxifen (44). The protein product of the oncogene c-Myc is an essential downstream effector of cell proliferation induced by the Wnt/β-catenin signaling pathway, and c-Myc is usually upregulated in various cancers (45). Xu *et al* (46) demonstrated that the LINC01094/miR-577 axis regulates the expression of β-catenin, c-Myc and cyclin D1 in ovarian cancer cells, thereby affecting the proliferation, migration, invasion and EMT of these cells. Another study showed that aspirin overcame tamoxifen resistance in estrogen receptor-positive breast cancer by downregulating c-Myc and cyclin D1 proteins (47). These reports, together with the results of the present study, support the hypothesis that TAX-resistant MCF-7 cell-derived exosome-delivered miR-187-5p regulates the viability, apoptosis, migration, invasion and colony formation of TAX-induced cells through the c-Myc/Wnt/β-catenin signaling pathway, thereby contributing to TAX resistance in breast cancer cells.

In conclusion, TAX-resistant cell-secreted exosome-delivered miR-187-5p promoted the viability, migration, invasion and colony formation of TAX-induced breast cancer cells while suppressing their apoptosis, thus conferring TAX resistance. The TAX resistance mechanism of exosomal miR-187-5p in breast cancer may be associated with the direct targeting of ABCD2 expression and the c-Myc/Wnt/β-catenin signaling pathway. Additional experiments using TAX-resistant breast cancer cells as positive controls will be conducted in the future to further validate the experimental results. The findings of the present study reveal the underlying mechanism of TAX resistance in breast cancer and suggest that exosomal miR-187-5p/ABCD2 and Wnt/β-catenin signaling are new potential targets and pathways for the treatment of patients with breast cancer who are resistant to TAX-based chemotherapy.

Acknowledgements

Not applicable.

Funding

No funding was received.

Availability of data and materials

The datasets used and/or analyzed during the current study are available from the corresponding author on reasonable request.

Authors' contributions

TW and QZ designed the experiments; TW, DZ, XW and NZ performed the experiments and analyzed the experimental results; QZ supervised the experiments; TW drafted the paper and QZ revised the manuscript. QZ and TW confirm the authenticity of all the raw data. All authors read and approved the final version of the manuscript.

Ethics approval and consent to participate

Not applicable.

Patient consent for publication

Not applicable.

Competing interests

The authors declare that they have no competing interests.

References

1. McDonald ES, Clark AS, Tchou J, Zhang P and Freedman GM: Clinical diagnosis and management of breast cancer. J Nucl Med 57 (Suppl 1): 9S-16S, 2016.
2. Gupta N, Gupta P and Srivastava SK: Penfluridol overcomes paclitaxel resistance in metastatic breast cancer. Sci Rep 9: 5066, 2019.
3. Siegel RL, Miller KD, Fuchs HE and Jemal A: Cancer statistics, 2021. CA Cancer J Clin 71: 7-33, 2021.
4. Hassan MS, Ansari J, Spooner D and Hussain SA: Chemotherapy for breast cancer (Review). Oncol Rep 24: 1121-1131, 2010.
5. Ghersi D, Willson ML, Chan MM, Simes J, Donoghue E and Wilcken N: Taxane-containing regimens for metastatic breast cancer. Cochrane Database Syst Rev 10: CD003366, 2015.

6. Megerdichian C, Olimpiadi Y and Hurvitz SA: nab-Paclitaxel in combination with biologically targeted agents for early and metastatic breast cancer. Cancer Treat Rev 40: 614-625, 2014.
7. Bukowski K, Kciuk M and Kontek R: Mechanisms of multidrug resistance in cancer chemotherapy. Int J Mol Sci 21: 3233, 2020.
8. Koual M, Tomkiewicz C, Cano-Sancho G, Antignac JP, Bats AS and Coumoul X: Environmental chemicals, breast cancer progression and drug resistance. Environ Health 19: 117, 2020.
9. Wang X, Li Z, Cui Y, Cui X, Chen C and Wang Z: Exosomes isolated from bone marrow mesenchymal stem cells exert a protective effect on osteoarthritis via lncRNA LYRM4-AS1-GRPR-miR-6515-5p. Front Cell Dev Biol 9: 644380, 2021.
10. Zhang L and Yu D: Exosomes in cancer development, metastasis, and immunity. Biochim Biophys Acta Rev Cancer 1871: 455-468, 2019.
11. Crow J, Atay S, Banskota S, Artale B, Schmitt S and Godwin AK: Exosomes as mediators of platinum resistance in ovarian cancer. Oncotarget 8: 11917-11936, 2017.
12. Yang F, Ning Z, Ma L, Liu W, Shao C, Shu Y and Shen H: Exosomal miRNAs and miRNA dysregulation in cancer-associated fibroblasts. Mol Cancer 16: 148, 2017.
13. Zhang J, Li S, Li L, Li M, Guo C, Yao J and Mi S: Exosome and exosomal microRNA: Trafficking, sorting, and function. Genomics Proteomics Bioinformatics 13: 17-24, 2015.
14. Ebert MS and Sharp PA: Roles for microRNAs in conferring robustness to biological processes. Cell 149: 515-524, 2012.
15. Geretto M, Pulliero A, Rosano C, Zhabayeva D, Bersimbaev R and Izzotti A: Resistance to cancer chemotherapeutic drugs is determined by pivotal microRNA regulators. Am J Cancer Res 7: 1350-1371, 2017.
16. Fu X, Liu M, Qu S, Ma J, Zhang Y, Shi T, Wen H, Yang Y, Wang S, Wang J, *et al*: Exosomal microRNA-32-5p induces multidrug resistance in hepatocellular carcinoma via the PI3K/Akt pathway. J Exp Clin Cancer Res 37: 52, 2018.
17. Fornari F, Pollutri D, Patrizi C, Bella TL, Marinelli S, Gardini AS, Marisi G, Toaldo MB, Baglioni M, Salvatore V, *et al*: In hepatocellular carcinoma miR-221 modulates sorafenib resistance through inhibition of caspase-3-mediated apoptosis. Clin Cancer Res 23: 3953-3965, 2017.
18. Uhr K, Prager-van der Smissen WJC, Heine AAJ, Ozturk B, van Jaarsveld MTM, Boersma AWM, Jager A, Wiemer EAC, Smid M, Foekens JA and Martens JWM: MicroRNAs as possible indicators of drug sensitivity in breast cancer cell lines. PLoS One 14: e0216400, 2019.
19. Thery C, Amigorena S, Raposo G and Clayton A: Isolation and characterization of exosomes from cell culture supernatants and biological fluids. Curr Protoc Cell Biol Chapter 3: Unit 3.22, 2006.
20. Lee YS, Kim SY, Ko E, Lee JH, Yi HS, Yoo YJ, Je J, Suh SJ, Jung YK, Kim JH, *et al*: Exosomes derived from palmitic acid-treated hepatocytes induce fibrotic activation of hepatic stellate cells. Sci Rep 7: 3710, 2017.
21. Martins TS, Catita J, Rosa IK, Silva OA and Henriques AG: Exosome isolation from distinct biofluids using precipitation and column-based approaches. PLoS One 13: e0198820, 2018.
22. Wu M, Ouyang Y, Wang Z, Zhang R, Huang PH, Chen C, Li H, Li P, Quinn D, Dao M, *et al*: Isolation of exosomes from whole blood by integrating acoustics and microfluidics. Proc Natl Acad Sci USA 114: 10584-10589, 2017.
23. Liao Z, Chen Y, Duan C, Zhu K, Huang R, Zhao H, Hintze M, Pu Q, Yuan Z, Lv L, *et al*: Cardiac telocytes inhibit cardiac microvascular endothelial cell apoptosis through exosomal miRNA-21-5p-targeted cdip1 silencing to improve angiogenesis following myocardial infarction. Theranostics 11: 268-291, 2021.
24. Yang C, Liu X, Zhao K, Zhu Y, Hu B, Zhou Y, Wang M, Wu Y, Zhang C, Xu J, *et al*: miRNA-21 promotes osteogenesis via the PTEN/PI3K/Akt/HIF-1alpha pathway and enhances bone regeneration in critical size defects. Stem Cell Res Ther 10: 65, 2019.
25. Livak KJ and Schmittgen TD: Analysis of relative gene expression data using real-time quantitative PCR and the 2(-Delta Delta C(T)) method. Methods 25: 402-408, 2001.
26. Park ST and Kim J: Trends in next-generation sequencing and a new era for whole genome sequencing. Int Neurourol J 20: S76-S83, 2016.
27. Kolak A, Kaminska M, Sygit K, Budny A, Surdyka D, Kukiełka-Budny B and Burdan F: Primary and secondary prevention of breast cancer. Ann Agric Environ Med 24: 549-553, 2017.
28. Denkert C, Liedtke C, Tutt A and von Minckwitz G: Molecular alterations in triple-negative breast cancer-the road to new treatment strategies. Lancet 389: 2430-2442, 2017.
29. Zhang S, Zhang H, Ghia EM, Huang J, Wu L, Zhang J, Lam S, Lei Y, He J, Cui B, *et al*: Inhibition of chemotherapy resistant breast cancer stem cells by a ROR1 specific antibody. Proc Natl Acad Sci U S A 116: 1370-1377, 2019.
30. Mashouri L, Yousefi H, Aref AR, Ahadi AM, Molaei F and Alahari SK: Exosomes: composition, biogenesis, and mechanisms in cancer metastasis and drug resistance. Mol Cancer 18: 75, 2019.
31. Santos JC, Lima NDS, Sarian LO, Matheu A, Ribeiro ML and Derchain SFM: Exosome-mediated breast cancer chemoresistance via miR-155 transfer. Sci Rep 8: 829, 2018.
32. Zheng P, Chen L, Yuan X, Luo Q, Liu Y, Xie G, Ma Y and Shen L: Exosomal transfer of tumor-associated macrophage-derived miR-21 confers cisplatin resistance in gastric cancer cells. J Exp Clin Cancer Res 36: 53, 2017.
33. Kampan NC, Madondo MT, McNally OM, Quinn M and Plebanski M: Paclitaxel and its evolving role in the management of ovarian cancer. Biomed Res Int 2015: 413076, 2015.
34. Weaver BA: How Taxol/paclitaxel kills cancer cells. Mol Biol Cell 25: 2677-2681, 2014.
35. Li Z, Lin C, Zhao L, Zhou L, Pan X, Quan J, Peng X, Li W, Li H, Xu J, *et al*: Oncogene miR-187-5p is associated with cellular proliferation, migration, invasion, apoptosis and an increased risk of recurrence in bladder cancer. Biomed Pharmacother 105: 461-469, 2018.
36. Hu YB, Yan C, Mu L, Mi YL, Zhao H, Hu H, Li XL, Tao DD, Wu YQ, Gong JP and Qin JC: Exosomal Wnt-induced dedifferentiation of colorectal cancer cells contributes to chemotherapy resistance. Oncogene 38: 1951-1965, 2019.
37. Qin X, Yu S, Zhou L, Shi M, Hu Y, Xu X, Shen B, Liu S, Yan D and Feng J: Cisplatin-resistant lung cancer cell-derived exosomes increase cisplatin resistance of recipient cells in exosomal miR-100-5p-dependent manner. Int J Nanomedicine 12: 3721-3733, 2017.
38. Dey N, Barwick BG, Moreno CS, Ordanic-Kodani M, Chen Z, Oprea-Ilies G, Tang W, Catzavelos C, Kerstann KF, Sledge GW Jr, *et al*: Wnt signaling in triple negative breast cancer is associated with metastasis. BMC Cancer 13: 537, 2013.
39. Hlavac V, Brynychova V, Vaclavikova R, Ehrlichová M, Vrána D, Pecha V, Koževnikovová R, Trnková M, Gatěk J, Kopperová D, *et al*: The expression profile of ATP-binding cassette transporter genes in breast carcinoma. Pharmacogenomics 14: 515-529, 2013.
40. Soucek P, Hlavac V, Elsnerova K, Vaclavikova R, Kozevnikovova R and Raus K: Whole exome sequencing analysis of ABCC8 and ABCD2 genes associating with clinical course of breast carcinoma. Physiol Res 64: S549-S557, 2015.
41. Park CY, Kim HS, Jang J, Lee H, Lee JS, Yoo JE, Lee DR and Kim DW: ABCD2 is a direct target of beta-catenin and TCF-4: Implications for X-linked adrenoleukodystrophy therapy. PLoS One 8: e56242, 2013.
42. Jia XX, Zhu TT, Huang Y, Zeng XX, Zhang H and Zhang WX: Wnt/β-catenin signaling pathway regulates asthma airway remodeling by influencing the expression of c-Myc and cyclin D1 via the p38 MAPK-dependent pathway. Exp Ther Med 18: 3431-3438, 2019.
43. Lin SY, Xia W, Wang JC, Kwong KY, Spohn B, Wen Y, Pestell RG and Hung MC: Beta-catenin, a novel prognostic marker for breast cancer: Its roles in cyclin D1 expression and cancer progression. Proc Natl Acad Sci USA 97: 4262-4266, 2000.
44. Shi Q, Li Y, Li S, Jin L, Lai H, Wu Y, Cai Z, Zhu M, Li Q, Li Y, *et al*: LncRNA DILA1 inhibits Cyclin D1 degradation and contributes to tamoxifen resistance in breast cancer. Nat Commun 11: 5513, 2020.
45. Gosens R, Baarsma HA, Heijink IH, Oenema TA, Halayko AJ, Meurs H and Schmidt M: De novo synthesis of {beta}-catenin via H-Ras and MEK regulates airway smooth muscle growth. FASEB J 24: 757-768, 2010.
46. Xu J, Zhang P, Sun H and Liu Y: LINC01094/miR-577 axis regulates the progression of ovarian cancer. J Ovarian Res 13: 122, 2020.
47. Cheng R, Liu YJ, Cui JW, Yang M, Liu XL, Li P, Wang Z, Zhu LZ, Lu SY, Zou L, *et al*: Aspirin regulation of c-myc and cyclinD1 proteins to overcome tamoxifen resistance in estrogen receptor-positive breast cancer cells. Oncotarget 8: 30252-30264, 2017.